

Preparation of a visibly photo-active $\text{TiO}_{2-x}\text{N}_x$ by planetary grinding of TiO_2 with NH_3 for an application in photocatalytic product design and manufacture

Jun-Bin Ko^a, Ki-Hyun Kim^b, Jae-Kil Han^c and In-Cheol Kang^{c,*}

^aHanbat University, San 16-1, Dukmyung-dong, Yuseong-gu, Daejeon, 305-719, Korea

^bJapan Fine Ceramics Center, 2-4-1 Mutsuno, Atsuta-ku, Nagoya 456-8587, Japan

^cSongdo TechnoPark, 7-50 Songdo-dong, Yeonsu-gu, Incheon 406-840, Republic of Korea

Nitrogen-doped TiO_2 (N-TiO_2), which shows a good photocatalytic activity to visible light irradiation, was successfully prepared by grinding TiO_2 with gaseous NH_3 . Nitrogen doping into TiO_2 induced narrowing of the band-gap, which resulted in more sensitive photo-activity to visible light irradiation. The procedure of nitrogen-doping was verified by X-ray photoelectron spectroscopy (XPS), NO_x decomposition activity, FT-IR spectrometry, UV-vis analysis and hydrogen detection results. The nitrogen doping was performed as follows, adsorption of gaseous NH_3 on TiO_2 surfaces and reaction with the activated surfaces of TiO_2 . New Ti-N bonds were generated before the breakage of N-H bonds of NH_3 adsorbed on TiO_2 . Finally, the prolonged grinding operation broke N-H bonds with the generation of H_2 , which resulted in the successful preparation of N doped TiO_2 .

Key words: Grinding, Nitrogen doping, TiO_2 Photocatalyst, NH_3 Gas.

Introduction

TiO_2 is considered to be a popular photocatalyst because of its good photo- and chemical stability, and excellent reactivity to UV-irradiation [1-3]. However, its weak reactivity under the visible light wavelength region due to the wide band-gap energy has limited its wide application. So, much effort such as on non-metal element or traditional metal element doping, and surface modification and complexation of the photocatalyst have been exhausted [4-10]. In particular, non-metal element doping studies have been a popular route in the preparation of a photo-active catalyst to visible light irradiation by narrowing the band-gap energy.

In general, anatase- TiO_2 shows better photocatalytic activity than rutile TiO_2 to ultraviolet irradiation because anatase TiO_2 has a higher specific surface area, and more surface-adsorbed water and hydroxyl groups than the rutile phase [11]. However, even anatase- TiO_2 shows no photocatalytic activity to visible light irradiation due to its wider band-gap energy (3.2 eV) compared with irradiation energy of visible light. On the other hand, TiO_2 doped with non metallic elements such as $\text{TiO}_{2-x}\text{N}_x$, $\text{TiO}_{2-x}\text{S}_x$, $\text{TiO}_{2-x}\text{C}_x$, have a sufficiently narrow band-gap energy to make electrons move from the valence band to the conduction band with visible light irradiation [5, 6, 12]. Structural defects such as lattice distortion with non metallic elements doping

resulted in a narrowing of band-gap energy. However, excess doping by non metallic elements might result in a decrease in the photocatalytic activity due to the change of chemical characteristics and an increase in the recombination rate of excited hole and electron pairs [13]. Therefore, adjusting to a suitable amount of doping might be the way forward.

It is not easy to dope non-metal elements into TiO_2 , because Ti-O bonding is more stable than that of Ti-N, Ti-C and Ti-S. As general methods for non-metal doping, sputtering, heat-treatment and oxidation of TiN at high temperature etc. have been used. [14-17]. However, these methods need expensive instruments, high temperature treatment and a delicate handling technique. By contrast, mechanochemical methods have been focused as a novel route for the preparation of composites, by pulverization, surface-modification, recycling etc. because they are simple processes, environmentally-friendly processes, economical processes, and operate at relatively low temperatures [6, 12].

In this study, TiO_2 was ground under an NH_3 ambient and heated in air at 200°C to prepare $\text{TiO}_{2-x}\text{N}_x$. The investigation carried on whether doping of N was successful or not, by studies the photocatalytic activity to visibly light irradiation and the nitrogen doping procedure based on the results of X-ray photoelectron spectroscopy (XPS), FT-IR spectrometry, UV-vis, and hydrogen detection. In addition, the nitrogen doping procedure was studied with a comparison of the results of a product ground with N_2 .

Experimental

Fig. 1 illustrates experimental flow. Anatase titania powder (a- TiO_2 , purity-min 98.5%, Wako Pure Chem., Inc., Japan)

*Corresponding author:
Tel : +82-32-260-0831
Fax : +82-32-260-0834
E-mail: kic22@step.or.kr

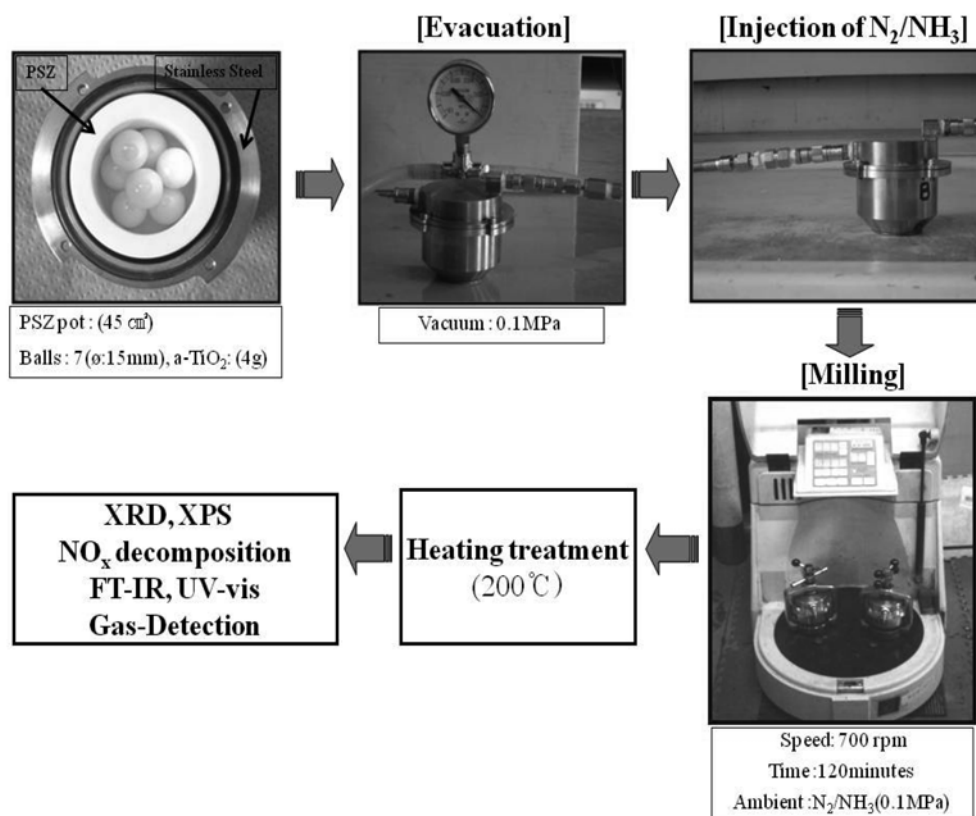


Fig. 1. Experimental flow.

was chosen as the starting material. A planetary ball mill (Pulverisette-7, Fritsch, Germany) was used for the grinding operation, which consisted of a set of pots (inside part) made of PSZ (partially stabilized zirconia) with an inner diameter of 45 cm³, and seven zirconia balls each with a diameter of 15 mm. Four grams of the TiO₂ powder and the seven balls were put into the pot, and NH₃ (purity 99.999%) or N₂ gas (purity 99.9%) was injected into the stainless steel pot (outside part) after the evacuation of the stainless steel pot reached 0.1 MPa. Then the grinding was performed at 700 rpm for two hours. The ground samples were heated at 200°C to remove chemical impurities adsorbed on the TiO₂ surfaces for 60 minutes in air.

The crystallinity of the ground products were analyzed by XRD (RAD-B, Rigaku Co. Ltd., Japan) to understand the influence of the grinding ambient (NH₃ and N₂) on the phase transition using Cu-K α radiation.

X-ray photoelectron spectroscopy (XPS) (PHI 5600 ESCA system, Ulvac-Phi, Inc., Japan) was conducted to record the surface chemical bonding energy of the products. This technique identifies whether nitrogen was successfully doped on to the TiO₂ or not. All products were sputtered with 3 kV Ar⁺ ion for 5 minutes on 4 × 4 mm² area, and the XPS scanning was recorded with Mg Ka X-ray by 20 times- 3cycles.

NO_x decomposition was examined to evaluate the photocatalytic activity under light in the visible wavelength region by measuring the concentration of NO_x gas at the

outlet of the reactor box (373 cm³) with a flow of 1 ppm NO-50 vol.% air mixed gas (200 cm³/minute). The product was placed on a glass holder plate with dimension 20 × 15 × 0.5 mm³ and set in the center of the reactor. A 450 W high-pressure mercury lamp was used to irradiate the product, where the wavelength was cut off with various filters such as a Pyrex glass to cut off the light of wavelength > 510 nm (Fuji's tri-acetyl cellulose filter), and > 400 nm (Kendo L41 Super Pro (W) filter).

The infrared spectra were recorded with an FT-IR spectrometer (FTS-40A, Bio-Rad) with the KBr disk method from 400 to 2000 wave-number (cm⁻¹) to analyze the chemical composition of surface.

UV-vis spectrophotometer (UV-2000, Shimadzu, Japan) was operated with a change of wavelength ranging from 700 to 200 nm to examine the optical absorbing edge of the products.

Hydrogen-detection was employed to determine whether hydrogen was generated or not during the grinding operation.

Results and Discussion

Fig. 2 represents the phase constitutions with a change of grinding ambient, which shows the influence of the grinding ambient on the phase transitions. Marks A, R and S indicate the anatase, rutile and srilankite phase of TiO₂. (a) is that of raw-TiO₂, which had just the anatase phase. By contrast, (d) ground in air has the rutile phase; almost

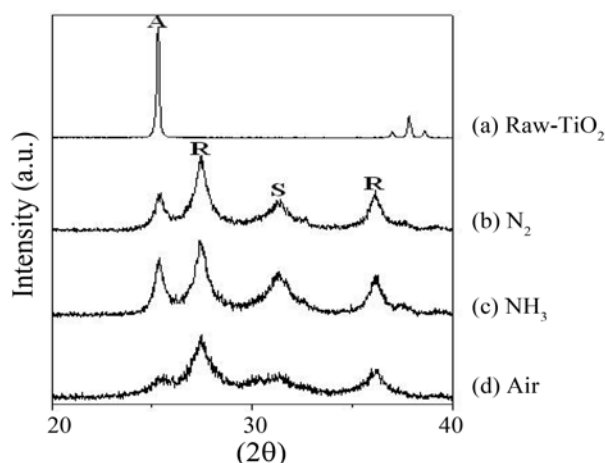


Fig. 2. Phase constitutions with grinding ambient; (a) raw-TiO₂, (b) N₂, (c) NH₃ and (d) Air. ((b), (c), (d) were ground at 700 rpm for 120 minutes followed by heat treatment at 200 °C for 60minutes in air).

all the anatase phase was changed into the rutile phase. This result means that mechanical energy could change anatase to rutile (the more stable phase) [6]. A comparison of (b), (c) and (d) identified that the grinding ambient resisted the rate of the phase transition; the rate of the phase transition with grinding under an NH₃ ambient was slower than N₂ (b) and air (d) ambient. It has been reported that it is easy to induce a phase transformation of TiO₂ with a low oxygen pressure during grinding because of the volume shrinkage due to oxygen deficiency [18]. However, the adsorption of the Lewis base NH₃ at fresh surfaces of TiO₂ caused a delay in the rate of the phase transition by reduction of the oxygen deficiency [18].

Fig. 3 shows the chemical binding energy of the products, which were recorded after surface sputtering with Ar⁺ ions. Result were obtained from (a) raw-TiO₂, (b) ground with N₂, and (c) ground with NH₃. The raw-TiO₂ and product (b) had any chemical binding energy with respect to nitrogen. On the other hand, product (c) showed two chemical bindings located at 396 eV and 400 eV. The 396 eV was assigned to the Ti-N binding energy [19], which means successful nitrogen doping into the oxygen sites of TiO₂. The 400 eV was assigned to the N-H and N-O chemical binding energies [20], which implied the existence of a few impurities such as NH₃ and NH₄⁺ on the surfaces of the product. The XPS results clearly demonstrated that the co-grinding of TiO₂ with NH₃ was effective to dope nitrogen into TiO₂, whereas N₂ was ineffective so to do, due probably to the chemical stable state of N₂.

The NO_x decomposition ability of each product was measured with a change of irradiation wavelength ranging above 510 nm and above 400 nm in wavelength (Fig. 4). The raw-TiO₂ showed no NO_x decomposition activity above the 510 nm wavelength region but showed decomposition activity of 14.5% above the 400 nm wavelength region. The product ground with N₂ gas showed no distinct enhancement of NO_x decomposition activity compared with raw-TiO₂ which was attributed to the failure of nitrogen

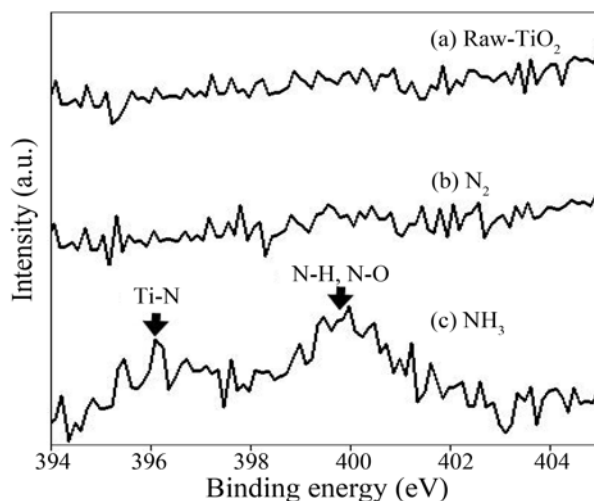


Fig. 3. XPS profiles of TiO₂ powders; (a) Raw-TiO₂, (b) ground with N₂ and (c) ground with NH₃.

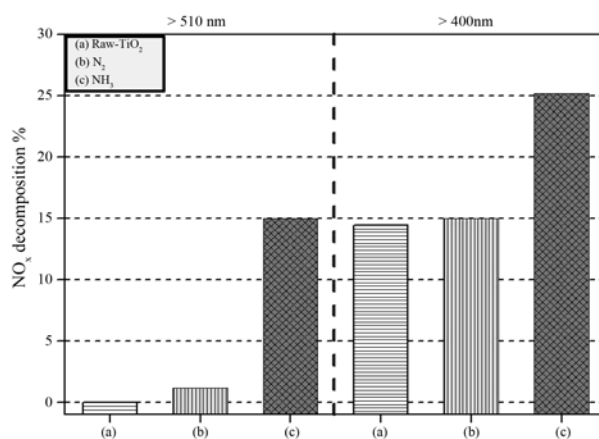


Fig. 4. NO_x decomposition activity with grinding ambients above 510 nm and 400 nm wavelengths; (a) Raw-TiO₂, (b) ground with N₂ and (c) ground with NH₃, respectively.

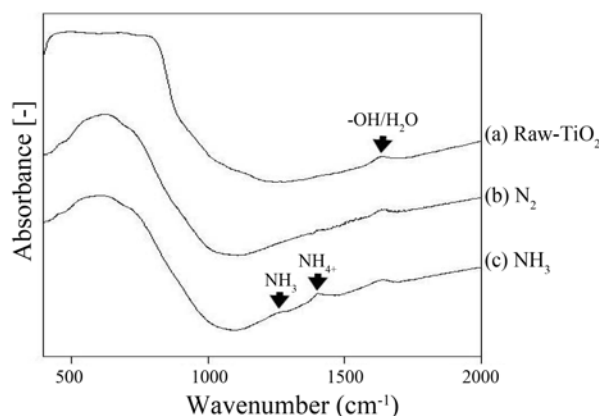


Fig. 5. FT-IR profiles with grinding ambients; (a) raw-TiO₂, (b) ground with N₂, (c) ground with NH₃, respectively.

doping into TiO₂. On the other hand, the product ground with NH₃ gas showed a distinctly improved NO_x decomposition activity compared with products (a) and (b), which was attributed to band-gap narrowing by nitrogen-doping.

These results agree well with the results from XPS in Fig. 3.

Fig. 5 demonstrates the surface chemical composition of products as a function of the grinding ambient. Hydroxyl groups and water were detected on the surfaces of all products. The product (b) ground with N_2 represented a similar surface chemical state to raw- TiO_2 (a). On the other hand, the product (c) ground with NH_3 showed NH_3 and NH_4^+ . The existence of these species was caused by a chemical bonding between NH_3 and Ti^{+4} , and between NH_3 and OH^- absorbed on TiO_2 surfaces during the grinding operation [21, 22]. These chemical bonds might be the beginning of the nitrogen doping procedure.

Fig. 6 represents optical absorbing edges with a change of grinding ambient. A raw- TiO_2 (a), which was inactive to the visible irradiation region, had one optical absorbing edge located at 380 nm in wavelength. The product (b) having anatase and rutile phases showed a shift of optical absorbing position towards the visible light region of 420 nm in wavelength, which was attributed to the generation of rutile- TiO_2 . The product (c) ground with NH_3 gas showed two optical absorbing edges positioned at 420 nm and 550 nm, which are assigned to band-gap narrowing via nitrogen doping and a phase transition by the grinding operation. From these results, it could be concluded that the co-grinding of TiO_2 with NH_3 resulted in band-gap narrowing via successful nitrogen doping, whereas the co-grinding of TiO_2 with N_2 was ineffective to dope with nitrogen.

Fig. 7 clearly verifies the generation of hydrogen gas after the grinding operation with NH_3 gas. Fig. 7(a) shows a color when hydrogen was absent, and Fig. 7(b) represents a color when hydrogen gas was present. The change of a yellowish color to dark blue implies that hydrogen gas was generated during the grinding operation under the

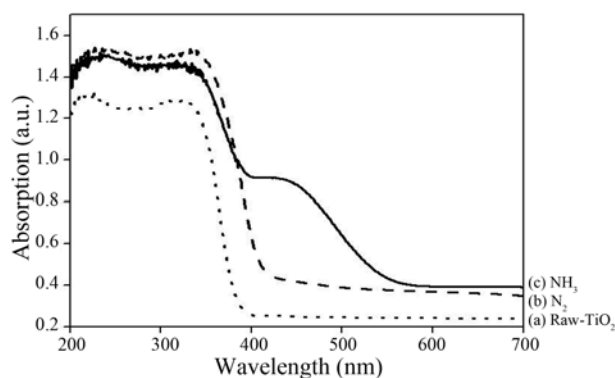


Fig. 6. UV-vis spectra profiles of TiO_2 powders; (a) raw- TiO_2 , (b) ground with N_2 , and (c) ground with NH_3 , respectively.



Fig. 7. The result of hydrogen-detection: (a) before and (b) after suction inside the pot ground with NH_3 .

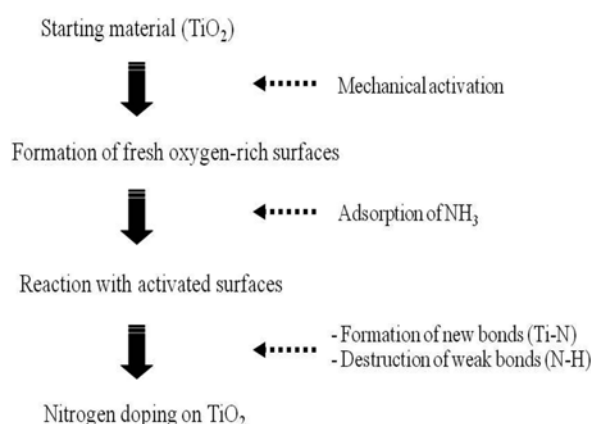


Fig. 8. Schematic flow of nitrogen doping procedure during the grinding operation of TiO_2 with NH_3 .

NH_3 ambient. This hydrogen gas might come from the breakage of the N-H bond of NH_3 .

With the results of Fig. 3, Fig. 4 and Fig. 6, it was proven that nitrogen doping by co-grinding with N_2 was impossible, because of the chemically stable state of N_2 . By contrast, the co-grinding TiO_2 with NH_3 made N-doping possible. Accordingly, taking into account the result of successful nitrogen doping into TiO_2 and the generation of hydrogen in co-grinding TiO_2 with NH_3 , it could be confirmed that nitrogen doping was realized before the breakage of the N-H bonds of NH_3 during the grinding operation.

Fig. 8 schematically illustrates the procedure of nitrogen doping into TiO_2 during the grinding operation with NH_3 . The mechanical activation by the grinding operation made fresh oxygen-rich surfaces on the TiO_2 . Then, Lewis base NH_3 adsorbed on the fresh surfaces of TiO_2 and reacted with the activate site Ti^{+4} of TiO_2 and resulted in the formation of new bonds (Ti-N) [18]. Further the N-H bonds of NH_3 were broken by the prolonged mechanical operation. Finally, nitrogen was successfully incorporated into TiO_2 , and hydrogen gas was generated.

Conclusions

Nitrogen doping into TiO_2 was successfully realized by a grinding operation of TiO_2 with gaseous NH_3 , which showed a good photocatalytic activity in the visible light wavelength region. On the other hand, grinding TiO_2 with N_2 was ineffective to dope N into TiO_2 because of the chemically stable state of N_2 .

The nitrogen doping proceeded as follows; fresh oxygen-rich surfaces were formed by mechanical activation. Gaseous NH_3 was adsorbed on the fresh oxygen-rich surfaces of TiO_2 and reacted with the activated surfaces, resulting in formation of new bonds (Ti-N). The weak bonds (N-H) in NH_3 adsorbed on the surfaces were broken by the prolonged grinding operation. Finally, it N doped TiO_2 was made. In other words, the nitrogen doping was realized not after the destruction of the N-H bonds of the NH_3 but before.

Acknowledgment

This research was supported by a grant from the Fundamental R&D Program for Core Technology of Materials funded by the Ministry of Knowledge Economy, Republic of Korea.

References

1. K.I. Hadjiivanov and D.K. Klissurski, *Chem. Soc. Rev.* 25 (1996) 61-69.
2. A. Heller, *Acc. Chem. Res.* 28 (1995) 503-508.
3. A. Linsebigler, G. Lu and J.T. Yates, *Chem. Rev.* 95 (1995) 735-738.
4. I.C. Kang, Q. Zhang, S. Yin, T. Sato and F. Saito, *Environ. Sci. Technol.* 42 (2008) 3622-3626.
5. Q. Zhang, J. Wang, S. Yin, T. Sato and F. Saito, *J. Am. Ceram. Soc.* 87 (2004) 1161-1163.
6. I.C. Kang, Q. Zhang, S. Yin, T. Sato and F. Saito, *Appl. Catalysis B: Environ.* 80 (2008) 81-87.
7. S. Klosek and D. Raftery, *J. Phys. Chem. B* 105 (2001) 2815-2819.
8. M. Anpo and M. Takeuchi, *J. Catal.* 216 (2003) 505-516.
9. J.C. Yu, J. Yu and J. Zhao, *Appl. Catal. B: Environ.* 36 (2002) 31-43.
10. I.C. Kang, Q. Zhang, S. Yin, T. Sato and F. Saito, *Appl. Catal. B: Environ.* 84 (2008) 570-576.
11. Z. Ding, G.Q. Lu, and P.F. Greenfield -*J. Phys. Chem. B* 104 (2000) 4815-4820.
12. S. Yin, K. Ihara, M. Komatsu, Q. Zhang, F. Saito, T. Kyotani and T. Sato, *Solid State Commu.* 137 (2006) 132-137.
13. H. Irie, Y. Watanabe and K. Hashimoto, *J. Phys. Chem. B* 107 (2003) 5483-5486.
14. W. Ren, Z. Ai, F. Jia, L. Zhang, X. Fan and Z. Zou, *Appl. Catal. B: Environ.* 69 (2007) 138-144.
15. M. Janus, M. Inagaki, B. Tryba, M. Toyoda and A.W. Morawski, *Appl. Catal. B: Environ.* 63 (2006) 272-276.
16. T. Lindgren, J. M. Mwabora, E. Avendano, J. Jonsson, A. Hoel, C.G. Granqvist and S.E. Lindquist, *J. Phys. Chem. B* 107 (2003) 5709-5716.
17. O. Diwald, T.L. Thompson, E.G. Goralski, S.D. Walck and J.T. Yates, *J. Phys. Chem. B* 108 (2004) 52-57.
18. G. Liu, F. Li, Z. Chen, G. Qing Lu and H.M. Cheng, *J. Solid State Chem.* 179 (2006) 331-335.
19. R. Asahi, T. Morikawa, T. Ohwaki, K. Aoki and Y. Taga, *Science* 293 (2001) 269-271.
20. N. C. Saha and H.G. Tompkins, *J. Appl. Phys.* 72 (1992) 3072-3079.
21. R. M. Pittman and Alexis T. Bell, *Catal. Lett.* 24 (1994) 1-13.
22. M. Hermann, H.P. Boehm and Z. Anorg. Allg. Chem. 368 (1969) 73-86.